Materials Letters 253 (2019) 250–254

Contents lists available at ScienceDirect

Materials Letters

journal homepage: www.elsevier.com/locate/mlblue

Reduced graphene oxide based supercapacitors: Study of self-discharge mechanisms, leakage current and stability via voltage holding tests

Rajneesh Kumar Mishra [a], Gyu Jin Choi [a], Youngku Sohn [b], Seung Hee Lee [c,*], Jin Seog Gwag [a,*]

[a] Department of Physics, Yeungnam University, Gyeongsan, Gyeongbuk 38541, South Korea
[b] Department of Chemistry, Chungnam National University, Daejeon, South Korea
[c] Applied Materials Institute for BIN Convergence, Department of BIN Convergence Technology and Department of Polymer-Nano Science and Technology, Chonbuk National University, Jeonju, Jeonbuk 561-756, South Korea

ARTICLE INFO

Article history:
Received 1 May 2019
Received in revised form 20 June 2019
Accepted 21 June 2019
Available online 22 June 2019

Keywords:
Reduced graphene oxide
Stability
Voltage holding tests
Self-discharge
Leakage current

ABSTRACT

Herein, we report the electrochemical properties such as self-discharge, leakage current and voltage holding tests (VHTs) of reduced graphene oxide (RGO) based solid-state symmetric supercapacitors (SSCs). SSC device demonstrates wide potential window (1.2 V), high specific capacity of 110.3 mA h g^{-1} at 1 A g^{-1}, high energy density of 22.1 W h kg^{-1} and ultra-high power density of 7304.5 W kg^{-1}. Further, SSC device depicts the high stability of 89.4% after 10,000 galvanostatic charge/discharge (GCD) cycles and 82.3% after 20 h VHTs. It also shows the small leakage current of 0.029 mA. Furthermore, SSC device retains the voltage of 0.7 V of its initial voltage (1.2 V) after 1 h self-discharge test, which suggests good state of health of the SSC device.

1. Introduction

Recently, the focus on the renewable energy storage devices has been extensively increased due to growing consumption of fossil fuels and ecological pollutions [1]. Supercapacitors have attracted vast interest due to their outstanding properties e.g. high power density (>10 kW kg^{-1}), quick charging-discharging, and excellent stability (via galvanostatic charging-discharging) and applications in electric vehicles, smart windows, wearable textile electronics, space exploration, self-powered electronic skins, and portable electronic gadgets, etc., [1–3]. However, it suffers desperately from the low energy density, which is also a serious issue, therefore, recently different two-dimensional nanomaterials have evolved and harnessed in the energy storage device [3,4]. In addition, the ion-accessible surface area is also immensely important and decisive to the capacitive performance than the physical surface area, due to inaccessible channels [5]. Therefore, the choice of electrode material is extremely important for the better ionic interactions in supercapacitors, which is significant to improve the specific capacitance and energy density without compromising with power density and long-term stability.

Among various carbon nanomaterials, reduced graphene oxide has attracted tremendous attention in recent years and is the well-known two-dimensional material composed of sp^2-hybridized carbon atoms with most enthralling mechanical, thermal, optoelectronics properties and excellent chemical stability [6]. Recently, many developments have been reported on fabrication of graphene based solid-state supercapacitor devices for energy harvesting applications such as multilayer graphene (58 mF cm^{-2} with stability of 84% after 10,000 cycles) [7], hybrid activated carbon/ electrochemically exfoliated graphene (59 F g^{-1} with stability of 96% after 60,000 cycles) [8], 3D graphene (170.6 A g^{-1} with stability of 86.2% after 10,000 cycles) [9]. Since, these above discussed reports have investigated the stability by galvanostatic charging-discharging (GCD) over 10,000 to 60,000 cycles, however these GCD tests for stability are not enough to commercialize the supercapacitor device in futuristic energy applications. Therefore, the voltage holding test (VHTs), self-discharge and leakage current are the vital parameters, which determine the state of health of the supercapacitor device needs to be further examined.

In this work, we demonstrated the reduced graphene oxide (RGO) based solid-state symmetric supercapacitor (SSC) device for energy storage applications. SSC device indicates the excellent stabilities via GCD cycling and voltage holding tests (VHTs). The self-discharge characteristics describes good health of SSC device and further provides the deep insight into two major

* Corresponding authors.
E-mail addresses: lsh1@jbnu.ac.kr (S.H. Lee), sweat3000@ynu.ac.kr (J.S. Gwag).

https://doi.org/10.1016/j.matlet.2019.06.073
0167-577X/

self-discharge mechanisms such as; (a) diffusion process and (b) leakage current through internal resistance.

2. Experimental details

Graphene oxide (GO) was synthesized from natural graphite (Alfa Aesar) using the modified Hummers method [10]. The reduced graphene oxide (RGO) was prepared by using the following procedure, first we added 500 mg of GO into the 500 mL of deionized (DI) water and kept under mild sonication to prepare good dissolution. Secondly, we added 1.75 mol of hydrazine hydrate into GO suspension and maintained temperature at 100 °C for 16 h under magnetic stirring, to finally get the black color RGO precipitate. This black precipitate was filtered, washed with DI water and ethanol, and dried in vacuum to receive RGO. The details of structural characterization techniques are discussed in the supporting information. The SSC device was fabricated by using two RGO electrodes, a separator (Whatman filter paper, grade 2), and electrolyte gel (PVA/Na_2SO_4). Na_2SO_4 is most commonly used as a neutral electrolyte solution due to low cost, greater safety and eco-friendly [10]. The SSC device fabrication details is discussed in the supporting information. The electrochemical properties of fabricated RGO based SSC device were studied by using an electrochemical workstation of Compactstat.h IVIUM Technologies. The electrochemical impedance spectroscopy (EIS) was performed in and open circuit potential in the frequency range from 1 Hz to 100 kHz.

3. Results and discussion

TEM images reveal the wrinkles, folded layers, and twisted layer surfaces of the reduced graphene oxide (RGO) as depicted in Fig. 1 (a–c), which predicts the possibilities of fast ionic interactions of electrolyte ions with RGO. Fig. 1(d) shows the HRTEM image, which illustrates the several overlapped and crossed lattice fringes. The inset in Fig. 1(d) shows fast Fourier transform (FFT) spectroscopy pattern corresponding to (0 0 2) lattice plane. Fig. 1(d_1 & d_2) shows the enlarged portion of HRTEM image and their corresponding FFT pattern, which illustrates the lattice spacing of 0.36 nm with (0 0 2) lattice plane. Fig. S1 shows the Raman

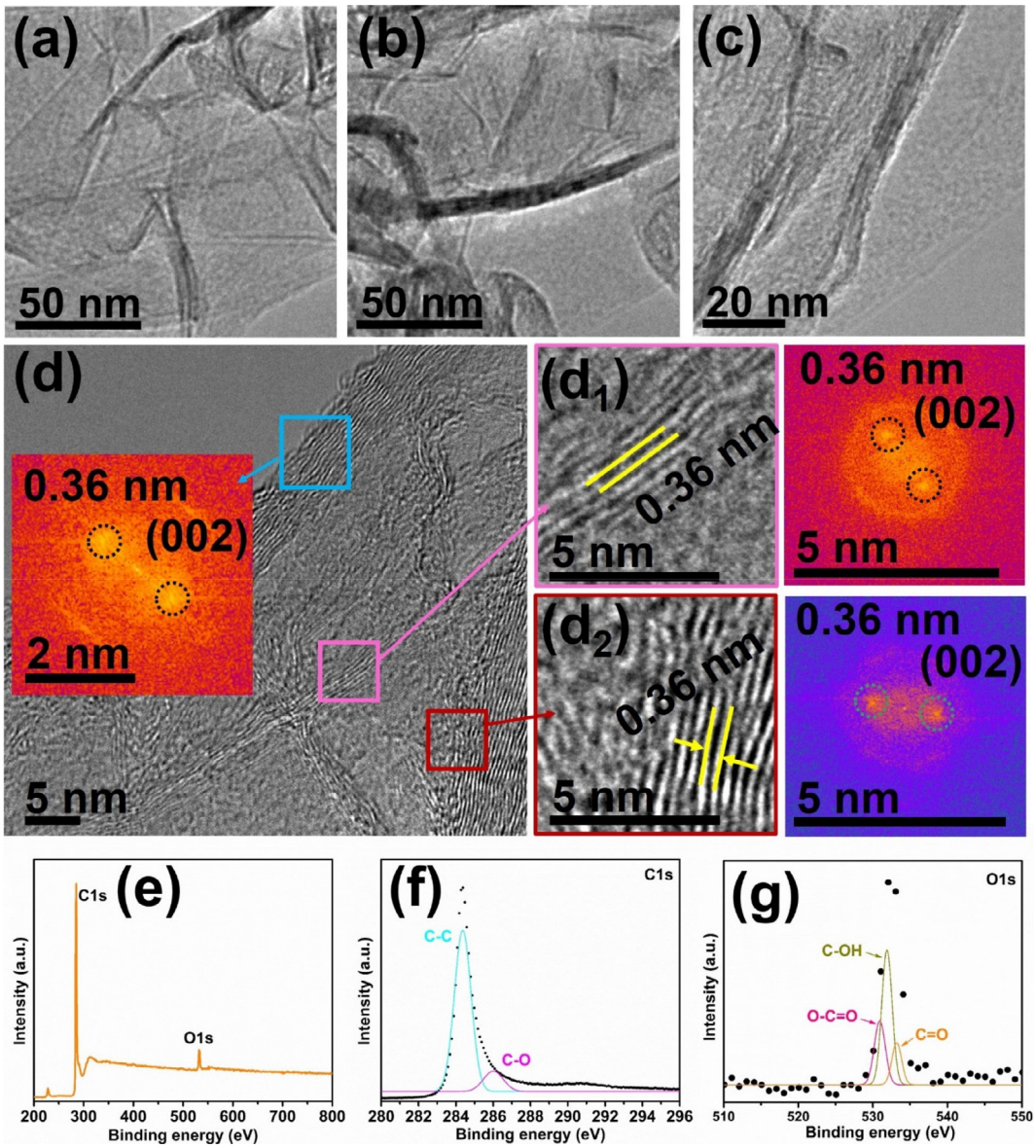

Fig. 1. (a–c) TEM, (d, d_1 and d_2) HRTEM image with corresponding FFT patterns, (e) XPS survey and narrow scan spectra (f) C1s and (g) O1s of RGO.

spectrum of RGO with prominent vibrational phonon modes at 1351.8 cm^{-1} [D band (A_{1g}) due to breathing modes of six-atom rings] and 1583.4 cm^{-1} [G band (E_{2g}) due to sp^2-bonded carbon atoms], respectively [11]. The intensity ratio of I_D/I_G is 0.60, which suggests that the synthesized RGO is multilayers (5–10 layers) [11]. Furthermore, the peaks at 284.7 eV and 532.1 eV in Fig. 1(e) are assigned to C1s and O1s of the RGO, respectively. Fig. 1(f) depicts the narrow scan XPS spectrum of C1s peak at 284.3 eV (C—C) and 286.1 eV (C—O) of RGO. Fig. 1(g) shows the narrow scan XPS spectrum of O1s peak at 530.9 eV (O—C=O), 531.8 eV (C—OH) and 533.2 eV (C=O) of RGO.

Fig. 2(a) displays the nearly rectangular shapes of cyclic voltammetry (CV) curves with wide potential window of 1.2 V, which reflect typically both the electrical double layer capacitance (EDLC) and pseudocapacitance behaviour. Fig. 2(b) estimates the value of slope *b* (evaluated by using Eq. S1) is 0.73 (found between 0.5 and 1), which indicates the involvement of both processes (i.e. capacitive and diffusion controlled processes) of charge storage kinetics [12]. Fig. 2(c) shows nonlinear behaviour of galvanostatic charge/ discharge (GCD) cycles at current density below 5 A g^{-1} and linear nature of GCD cycles at current density above 5 A g^{-1}, because of electrical double layer capacitance (EDLC) and pseudocapacitance nature, which gestures the superior charge storage reversibility of SSC device [12]. Fig. 2(d) shows the high and low specific capacity (evaluated by using Eq. S2) 110.3 mA h g^{-1} at 1 A g^{-1} and 77.7 mA0 h g^{-1} at 15 A g^{-1}, respectively. Fig. 2(e) illustrates high energy density 22.1 W h kg^{-1}, (evaluated by using Eq. S3) and excellent power density 7304.5 W kg^{-1} (evaluated by using Eq. S4). Fig. 2(f) shows the excellent stability of 89.4% after 10,000 GCD cycles. This high stability is due to the layered structure, high surface area and good conductivity of RGO, which provides efficient pathways of electron transport and enhances the rate capability [13].

Fig. 3(a) elucidates the voltage holding tests (VHTs) at 1.2 V after charging at 5 A g^{-1} (inset shows 4 cycles of GCD cycles before/after VHTs). Overall, we performed VHTs of SSC device over 20 h. In Fig. 3(b), the specific capacity fluctuates up to initial 6 h and afterwards it reduces to 71.8 mA h g^{-1} from 87.3 mA h g^{-1} during 20 h VHTs, which results high rate capability (87.2%) of the SSC device. The SSC device delivered the excellent stability of 82.3% after 20 h VHTs. The leakage current was recorded during VHTs as shown in Fig. 3(c). Leakage current diminishes significantly to 0.039 mA within few seconds and then it further reduces its low value of 0.029 mA. After 10,000 GCD cycles and 20 h VHTs, we performed self-discharge test of same SSC device for one hour. Fig. 3(d) displays the good capability of 0.7 V after 1 h self-discharge test. The two well-known models were taken into account such as (a) leakage current through internal resistance (Eq. S5) and (b) the diffusion-controlled process (Eq. S6). Fig. S2 displays the nonlinear plot and is not well fitted with Eq. S5, therefore, it predicts that the self-discharge phenomena is not due to leakage current through internal resistance. However, Fig. 6(e) illustrates the self-discharge characteristics of SSC device, which is well fitted with Eq. S6 and validates that the self-discharge is mainly due to diffusion controlled-process.

From Fig. 3(f), the values of internal (R_s) are 2.9 Ω/ 4.9 Ω, charge transfer resistances (R_{ct}) are 1.0 Ω/ 1.2 Ω, Warburg impedance (Z_w) are 6.2 Ω/ 8.9 Ω before/ after 10,000 GCD cycles & 20 VHTs, respectively, which contributes in the diffusion of electrolyte ions during redox reactions (inset shows the equivalent circuit model) [14]. In addition, SSC device shows asymmetrical behaviour of the EIS spectra, which may be due to 20 h voltage holding tests even after 10,000 GCD cycles. Fig. 3(g) shows the Randles plots, which provides the value of Warburg coefficient (σ) [13.1/17.0 before/after 10,000 GCD cycles and 20 h VHTs, evaluated by using Eq. S7] and justified the insights of the diffusion processes. Fig. S3 shows the imaginary part of Randles plots and discussed in the Supporting information. Fig. 3(h) shows Bode plots with phase angles of – 74.8° and – 69.3° at the frequencies of 0.81 Hz and 0.68 Hz before/ after 10,000 GCD cycles and 20 h VHTs, respectively. To demonstrate the applicability of supercapacitor device, three RGO based SSC device are connected in series to produce a voltage of ~4.9 V as shown in Fig. 3(i). After charging, they can illuminate a green light emitting diode (LED) for more than 3 minutes. Furthermore, it is found that the single SSC device cannot illuminate a green LED due to low RGO loading (1.5 mg per SSC device). In

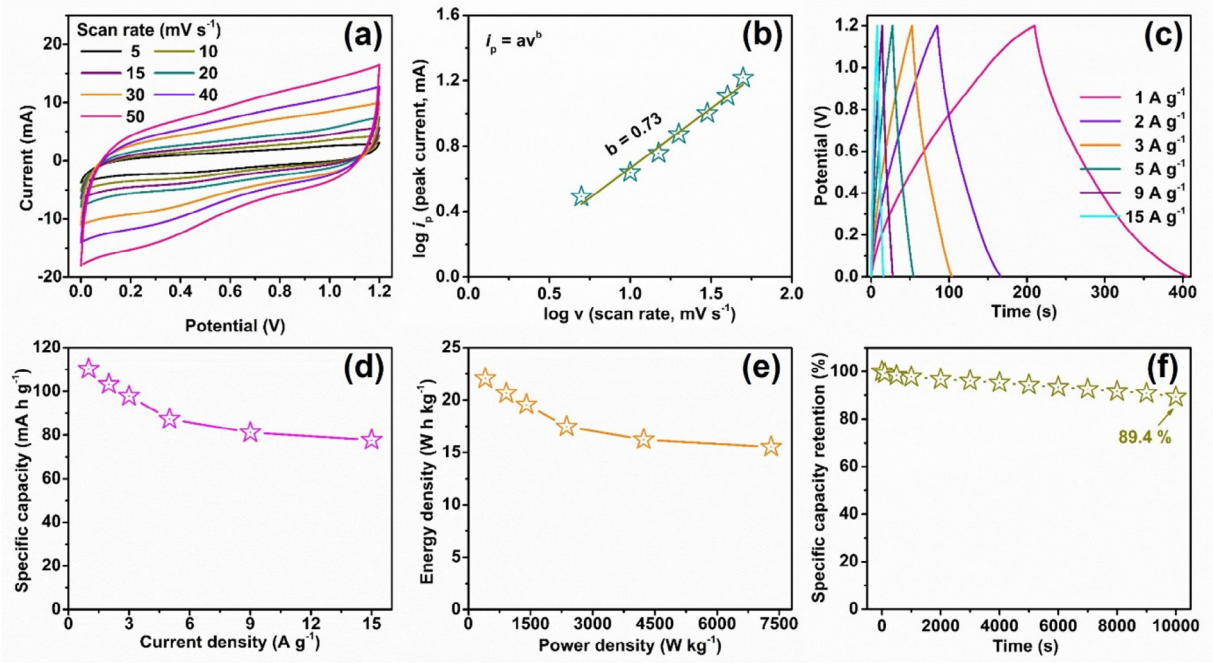

Fig. 2. RGO based SSC device; (a) CV, (b) log i_p vs log *v* plot, (c) GCD cycles, (d) specific capacity, (e) energy density vs power density (Ragone plots) and (f) stability at 5 A g^{-1}.

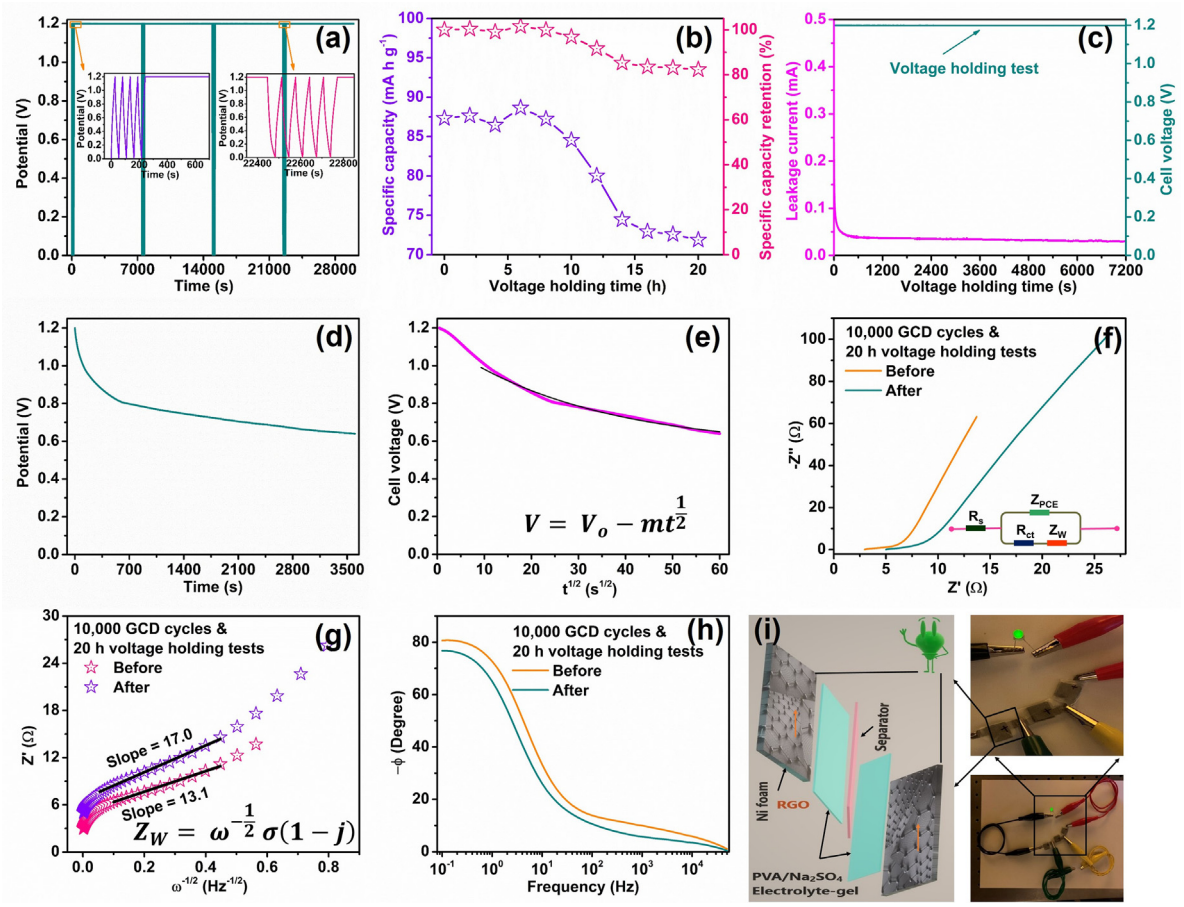

Fig. 3. RGO based SSC device; (a) VHTs at 1.2 V, (b) specific capacity & stability at 5 A g^{-1}, (c) leakage current, (d) self-discharge, (e) diffusion-controlled process (self-discharge mechanism), (f) impedance spectra, (g) Randles & (h) Bode plots and (i) demonstration of green LED illumination.

addition, we discussed a comparative study of RGO and RGO composites as electrode materials for supercapacitor device applications as shown in Table S1 in the supporting information.

4. Conclusions

The SSC device demonstrates excellent stability of 89.4% and 82.3% evaluated by both the 10,000 GCD cycles and 20 h voltage holding tests, respectively. Furthermore, the self-discharge characteristics of SSC device verifies the dominant nature of diffusion process over leakage current through the internal resistance. Therefore, RGO based SSC device with notable electrochemical properties could be futuristic materials for the next-generation energy storage devices applications.

Declaration of Competing Interest

None.

Acknowledgements

This work was supported through the Basic Science Research Program through the National Research foundation of Korea (NRF) funded by the Ministry of Science, ICT, and Future Planning (Grant No. 2016R1D1A3B03932396).

Appendix A. Supplementary data

Supplementary data to this article can be found online at https://doi.org/10.1016/j.matlet.2019.06.073.

References

[1] (a) Y. Zhong, Z. Chai, Z. Liang, P. Sun, W. Xie, C. Zhao, W. Mai, ACS Appl. Mater. Interfaces 9 (2017) 34085–34092;
(b) B.Y. Guan, L. Yu, X. Wang, S. Song, X.W. (David) Lou, Adv. Mater. 29 (2017) 1605051.
[2] K. Jost, G. Dion, Y. Gogotsi, J. Mater. Chem. A 2 (2014) 10776–10787.
[3] (a) B.Y. Guan, X.Y. Yu, H.B. Wu, X.W. (David) Lou, Adv. Mater. 29 (2017) 1703614;
(b) R.K. Mishra, J.H. Ryu, H.-In Kwon, S.H. Jin, J. Mater. Chem. A 6 (2018) 15253–15264.
[4] C. Huang, J. Zhang, N.P. Young, H.J. Snaith, P.S. Grant, Sci. Rep. 6 (2016) 25684.
[5] Z.X. Mao, C. Wang, Q. Shan, M.J. Wang, Y. Zhang, W. Ding, S. Chen, L. Li, J. Li, Z. Wei, J. Mater. Chem. A 6 (2018) 8868–8873.
[6] Y. Zhou, P. Jin, Y. Zhou, Y. Zhu, Sci. Rep. 8 (2018) 9005.
[7] G. de S. Augusto, J. Scarmínio, P.R.C. Silva, A. de Siervo, C.S. Rout, F. Rouxinol, R. V. Gelamo, Electrochim. Acta 285 (2018) 241–253.
[8] I.-L. Tsai, J. Cao, L.L. Fevre, B. Wang, R. Todd, R.A.W. Dryfe, A.J. Forsyth, Electrochim. Acta 257 (2017) 372–379.
[9] X. Liu, S. Zou, K. Liu, C. Lv, Z. Wu, Y. Yin, T. Liang, Z. Xie, J. Power Sources 384 (2018) 214–222.
[10] (a) J. Chen, B. Yao, C. Li, G. Shi, Carbon 64 (2013) 225–229;
(b) K. Fic, M. Meller, J. Menzel, E. Frackowiak, Electrochim. Acta 206 (2016) 496–503.
[11] (a) C. Ferrante, A. Virga, L. Benfatto, M. Martinati, D. De Fazio, U. Sassi, C. Fasolato, A.K. Ott, P. Postorino, D. Yoon, G. Cerullo, F. Mauri, A.C. Ferrari, T. Scopigno, Nat. Commun. 9 (2018) 308;
(b) B.V. Lopez, R.S. Sundaram, C.G. Navarro, D. Olea, M. Burghard, J.G. Herrero, F. Zamora, K. Kern, Adv. Mater. 21 (2009) 4683–4686.

[12] (a) B.Y. Guan, A. Kushima, L. Yu, S. Li, J. Li, X.W. (David) Lou, Adv. Mater. 29 (2017) 1605902;
(b) J. Du, L. Liu, Y. Yu, L. Zhang, Y. Zhang, A. Chen, Mater. Chem. Phys. 223 (2019) 145–151.
[13] W. Fu, Y. Zhao, J. Mei, F. Wang, W. Han, F. Wang, E. Xie, Electrochim. Acta 283 (2018) 737–743.
[14] J. Song, Y. Chen, K. Cao, Y. Lu, J.H. Xin, X. Tao, ACS Appl. Mater. Interfaces 10 (2018) 39839–39850.